International Journal of Remote Sensing
Vol. 00, No. 00, DD Month 200x, 1–8

Letter

Wide Band SAR Sub-Band Splitting and Inter-Band Coherence Measurements

D. DERAUW*†‡ , A. ORBAN† and Ch. BARBIER†

†Centre Spatial de Liège, Avenue du Pré-Aily, 4031 Angleur, Belgium
‡ Royal Military Academy, Avenue de la Renaissancelaan, 1000 Brussels, Belgium

(*April 2009*)

Range resolution of SAR images is determined by transmitted radar signal bandwidth. Most recent SAR sensors use wide band signals in order to achieve metric range resolution, while metric azimuth resolution can be achieved in spotlight mode. As an example, ENVISAT ASAR sensor uses a 15 MHz bandwidth chirp while TerraSAR-X spotlight mode uses signals having 150 MHz bandwidth leading to a potentially 10 times higher resolution. One can also take advantage of wide band to split the full band into sub-bands and generate several lower resolution images from a single acquisition, each being centred on slightly different frequencies. These sub-images can then be used in a classical interferometric process to measure inter-band coherence of a given scene. This inter-band coherence reveals scatterers keeping a stable phase behaviour along with frequency shift. A simple coherence model derived from Zebker model for randomly distributed surface scatterers is proposed. Examples are presented, showing that scatterers can have a behaviour that deviates from the model, leading to a new information channel.

1. Introduction

Recently-launched SAR sensors like TerraSAR-X or CosmoSkyMed are equipped with wide bandwidth radar signal emitters. Working at large bandwidth allows metric range resolution, which combined with spotlight mode, leads to Very High Resolution (VHR) SAR imagery.

Wide band signals also provide a supplementary degree of freedom that is expected to be useful for absolute ranging (Bamler *et al.* 2004). In VHR SAR, the ratio between the carrier wavelength and resolution cell is about 50 for civilian space-borne SAR missions and up to 15 in the case of sub-metric airborne SAR sensors. Nevertheless, through interferometric processing, absolute ranging can only be performed ambiguously, within a phase cycle.

The new degree of freedom offered by wide band signals allows this ambiguity to be removed. The principle was already proposed by Masden and Zebker (Madsen *et al.* 1992) using two sub-band interferograms as a possible solution for absolute phase unwrapping. The principle can be extended, segmenting the full wide band into sub-bands and generating several lower range resolution sub-images, each centred on a different frequency. Generating these *chromatic views* for each image of an interferometric pair allows generating as many interferograms, each having

*Corresponding author. Email: dderauw@ulg.ac.be

International Journal of Remote Sensing
ISSN 0143-1161 print / ISSN 1366-5901 online © 200x Taylor & Francis
http://www.tandf.co.uk/journals
DOI: 10.1080/0143116YYxxxxxxxx

a different carrier frequency.

Scatterers keeping a coherent behaviour in each sub-band interferogram show a phase that varies linearly with the central frequency, the slope being proportional to the absolute optical path difference. This potentially solves the problem of phase unwrapping on a pixel by pixel basis (Veneziani *et al.* 2003, Bamler *et al.* 2004, 2005).

All the above aspects are currently being addressed in an *ESA* project entitled Wide band Multi-Chromatic Assessment (*WiMCA*) carried out by the Istituto di Studi sui Sistemi Intelligenti per l'Automazione – Bari, Italy (*ISSIA – CNR*), *TELESPAZIO* – Rome, Italy and Centre Spatial de Liège – Belgium (*CSL*).

The *frequency-coherent* scatterers are defined operationally as those pixels where the phase in the multi-frequency interferograms show a linear behaviour. Analogously to the temporal Persistent Scatterers (Ferretti *et al.* 2001), coherence thresholds can be used to define reliable scatterers (Veneziani *et al.* 2006) for split band interferometric processing.

In this letter, an innovative aspect studied in the frame of the *WiMCA* project and aiming at analyzing the information content within a single wide band SAR acquisition is adressed.

Sub-band splitting of a single wide band acquisition will give chromatic views of the scene, each centered on a different carrier frequency, and each observing the same on-ground scatterer distribution. One can thus measure decorrelation between pairs of chromatic views through a classical interferometric process.

First, a simple coherence model derived from the Zebker model (Zebker *et al.* 1992) is proposed, showing that, for randomly distributed surface scatterers, coherence should fall to zero for non-overlapping sub-bands.

Second, an example using a *TerraSAR-X* acquisition is presented, showing that inter-band coherence may deviate from this simple model. This is a consequence of the fact that observed scatterer distributions may differ locally from the underlying hypothesis of the model (i.e. randomly distributed surface scatterers). As a consequence, inter-band coherence bears information related to the scatterer distribution and to the scattering process within the resolution cell.

2. Adapted Zebker Model

Considering classical SAR interferometry in a monostatic configuration, two signals s_1 and s_2 are acquired by a single antenna observing the same area in two successive passes. If x and y are respectively the azimuth and ground range coordinates, the measured signals in the final processed images, at the position (x_0, y_0), are expressed by (Zebker *et al.* 1992):

$$s_1 = \iint f\left(x - x_0, y - y_0\right) e^{-j\frac{4\pi}{\lambda}(r + y sin(\theta_1))} W\left(x, y\right) dxdy + n_1 \tag{1a}$$

$$s_2 = \iint f\left(x - x_0, y - y_0\right) e^{-j\frac{4\pi}{\lambda}(r + y sin(\theta_2))} W\left(x, y\right) dxdy + n_2 \tag{1b}$$

where r is the slant range to the considered point at position (x_0, y_0), $f(x, y)$ represents the complex backscatter function of each point of the surface and $W(x, y)$ is the point target response of the acquisition system. n_i is the noise associated with each receiver. The angles θ_1 and θ_2 are the local incidence angles of the radar signals as depicted in figure 1.

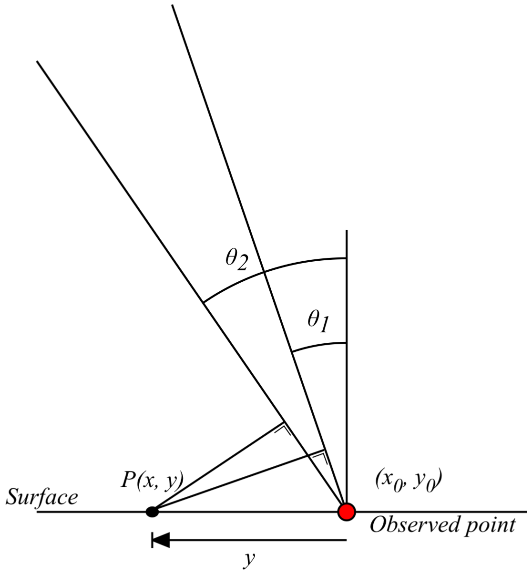

Figure 1. Schematic interferometric SAR viewing geometry

The interferometric process is described through the cross-correlation of the two signals s_1 and s_2, i.e., $\langle s_1 s_2^* \rangle$

In the Zebker model, uniformly distributed and uncorrelated surface scattering centres are assumed. Considering in addition a classical sinc impulse response, this cross-correlation is readily obtained.

Evaluation of the cross-correlation followed by normalization leads to the well-known expression for the geometrical decorrelation function (Zebker *et al.* 1992):

$$\gamma = 1 - 2R_y \left(\frac{sin(\theta_1)}{\lambda} - \frac{sin(\theta_2)}{\lambda} \right) \simeq 1 - \frac{2cos(\theta)|\delta\theta| R_y}{\lambda} \tag{2}$$

where R_y is the range resolution of the system θ is the average of the incidence angles and $\delta\theta = \theta_1 - \theta_2$.

Equation 2 allows the critical baseline inducing complete geometrical decorrelation to be determined in the presence of randomly distributed surface scatterers.

Now, adapting the model to sub-band interferometry, one considers a single viewing angle θ, but two wavelengths λ_1 and λ_2. Therefore, the expression for coherence γ becomes:

$$\gamma = 1 - 2R_y sin(\theta)\left(\frac{1}{\lambda_1} - \frac{1}{\lambda_2}\right) \tag{3}$$

Using:

$$R_y sin(\theta) = \delta r = \frac{c}{2B} \tag{4}$$

the relation giving the range resolution δr with respect to the signal bandwidth B and expressing equations in terms of central frequencies finally leads to:

$$\gamma = 1 - \frac{\Delta\nu}{B} \tag{5}$$

where $\Delta\nu$ is sub-bands central frequencies separation.
Similarly to the critical baseline leading to full coherence loss in classical InSAR, inter-band coherence is completely lost when the sub-band separation equals their bandwidth i.e. when $\Delta\nu = B$. An identical result can be obtained readily considering the Just & Bamler formalism (Just *et al.* 1994).

3. Inter-Band Coherence Measurement

3.1 *Data Set*

A TerraSAR-X spotlight interferometric pair was downloaded from the InfoTerra web site. This data set is made of two spotlight Single Look Complex images of Bergen, Norway acquired on November 24 and December 5, 2007. The available bandwidth is 150MHz.

First, a classical interferometric process was performed to derive the interferometric coherence on the whole scene. Interferometric coherence along with the corresponding histogram and an amplitude image of the whole scene is represented in figure 2.

3.2 *Sub-Band Splitting and Inter-Band Coherence Measurements*

In a second step, sub-band splitting of the first acquisition considered as master in the interferometric pair was performed. A de-Hamming filter was first applied to the whole data in the Fourier domain. In the case of TerraSAR-X data, the applied Hamming filter has an apodization coefficient of 0.6 for all modes (in place of 0.56 as strictly defined for Hamming window). Depending on user parameters, the sub-band filter is generated and centered on requested central frequencies in the Fourier domain to generate each chromatic view.

Seven chromatic views were generated, each having a 40 MHz sub-band bandwidth with central frequencies spaced every 18.88 MHz before and after the central frequency of the full resolution image. Consequently, each sub-band partially overlaps the preceding and the next one by about 53%. Overlapping with the second preceding and the second next is about 5%. No overlap occurs between the others sub-bands.

(a)
(b)

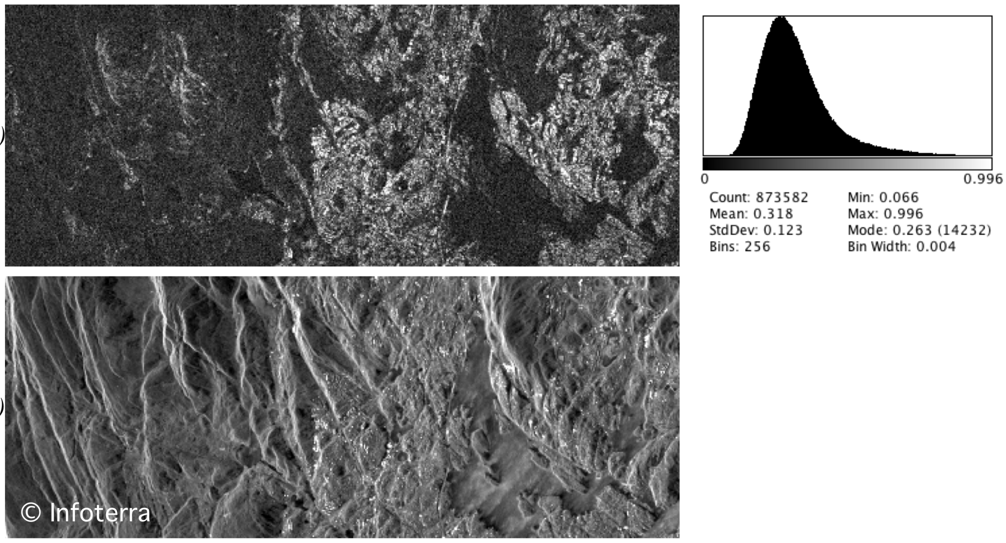

Figure 2. (a): Interferometric coherence and corresponding histogram
(b): Amplitude image of the observed scene.

Having seven sub-views of this TerraSAR-X spotlight acquisition, inter-band interferometry processing was performed to evaluate the coherence between sub-views of a same image. Seven sub-views allow 21 potential interferometric pairs to be generated.

Whatever the sub-view considered as master image, the results appear to be the same: coherence remains partially preserved when performing interferometry with the sub-view obtained from sub-bands immediately on the left or on the right of the reference one. Then, globally, coherence rapidly decreases with central frequencies gap but some areas keep a high level of coherence even if there is no overlap between sub-bands.

Figure 3 shows the 6 inter-band coherence images obtained considering the sub-view centred on the full resolution carrier frequency as master. Slave sub-view central frequency increases from bottom to top of the figure. Corresponding histograms are shown on the left of each coherence image.

Figures *3(d)* and *3(c)* are obtained considering respectively slave sub-views just before and just after the master one in terms of sub-band central frequencies. For those sub-views, spectra overlap partially by about 53%. As can be seen, histograms average values are very close to that value. It is thus in good agreement with the adapted Zebker model and derived equation 5.

When the sub-bands overlap is of only a few percent, coherence still decreases but not to the expected level. Some clearly scene-related structures appear, some points keeping a quite high coherence level. Even when there is no overlap between sub-bands, coherence does not fall to zero as expected from the theoretical model. The same structures stay still well observable. One can also observe that this inter-band coherence appears roughly similar to the interferometric coherence in figure 2.

The fact that coherence does not fall to zero with sub-band separation as expected from the model may have several origins:

- The coherence is not measured but estimated and it is well known that co-

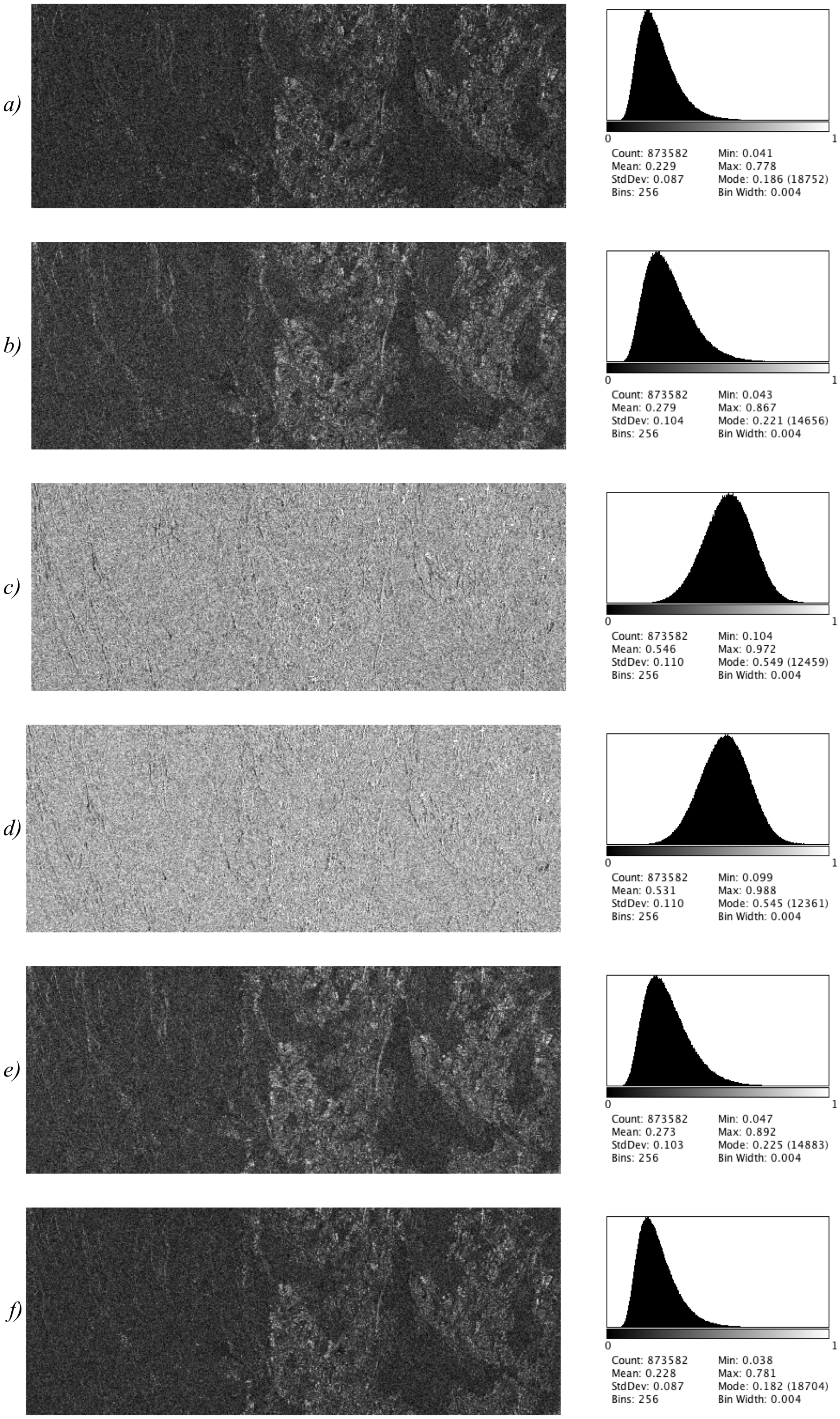

Figure 3. Inter band coherence measurements with corresponding histograms

herence estimators are biased. The estimation is only correct for a coherence of 1. This bias is clearly visible on coherence histograms; the minimum value never falls below 4%.

- The model is valid only for random surface scatterers. The observed surface cannot be considered as purely made of random surface scatterers. There are forested areas in which volume scattering dominates and also urban areas in which dihedral scattering process dominates. Moreover, the considered scene is a spotlight scene with a very high spatial resolution. In such a metric resolution cell, distribution randomness of scatterers with respect to the wavelength is less granted than with classical resolution sensors like ERS or ENVISAT offering a resolution cell having an area 100 times larger.

The fact that the model fails to describe a real scene is interesting in the sense that deviation with respect to random surface scattering reveals other scatterer distributions and scattering processes. Consequently, inter-band coherence, like interferometric coherence, can be considered as an information channel related to local scatterer distributions and scattering processes; this information channel being extracted from a single acquisition.

Considering possible deviation with respect to the main hypothesis (i.e. random distribution of surface scatterers), inter-band coherence should allow to discriminate volume or dihedral scattering processes from surface scattering. Tests are currently being performed to analyse the ability to use inter-band coherence in marine surveillance, for example, using coherence level to discriminate vessels from the surrounding sea in a single wide band SAR acquisition. A similar approach was proposed by Ouchi (Ouchi *et al.* 2004), using cross correlation of amplitude sub-look images issued from a single SAR acquisition. In that case, sub-band splitting is performed on the azimuth spectra.

4. Conclusions

Information content of a wide band SAR acquisition through sub-band splitting and inter-band coherence measurements was studied. The Zebker model proposed for classical InSAR was adapted to describe inter-band coherence. With respect to this simple model, coherence should stay proportional to sub-band overlap. Dis crepancies with respect to this simple model were observed splitting a TerraSAR-X spotlight acquisition into seven sub-views and performing inter-band coherence measurements. Coherence decreases, but does not fall to zero as expected. As in interferometric coherence, inter-band coherence reveals scene related features. Inter-band coherence can thus be considered as an information channel related to local scatterer distributions and scattering processes; this information channel being extracted from a single wide band SAR acquisition.

5. Acknowledgments

This work was carried out under ESA contract No 21319/07/NL/HE. The authors acknowledge helpful discussions with Rafaël Vitulli (*ESA*) and Dr Veneziani (*ISSIA*).

References

Bamler, R. and Eineder, M., 2004, Split Band Interferometry versus Absolute Ranging with Wideband SAR Systems. In *Proceedings of the International Geoscience & Remote Sensing Symposium (IGARSS'04)*, Vol. II, pp. 980-984.

Bamler, R. and Eineder, M., 2005, Accuracy of Differential Shift Estimation by Correlation and Split-Bandwidth Interferometry for Wideband and Delta-k SAR Systems. *IEEE Geoscience and Remote Sensing Letters*, **2**(2), pp. 151-155.

Ferretti, A., Prati, C. and Rocca, F., 2001, Permanent Scatterers in SAR Interferometry. *IEEE Transactions in Geosciences and Remote Sensing*, **39**(1), pp. 8-20.

Just, D. and Bamler, R., 1994, Phase Statistics of Interferograms with Application to Synthetic Aperture Radar. *Applied Optics* **33**(20), pp. 4361–4368.

Madsen, S.N. and Zebker, H.A., 1992, Automated Absolute Phase Retrieval in Across-Track Interferometry. In *Proceedings of the International Geoscience & Remote Sensing Symposium (IGARSS'92)*, Vol. II, pp. 1582-1584.

Ouchi, K., Tamaki, S., Yagushi, H. and Iehara, M., 2004, Ship detection based on coherence lags derived from cross-correlation of mulilook SAR images. *IEEE Geosciences and Remote Sensing Letters*, **1**(3), pp. 184-187.

Veneziani, N., Bovenga, F., Refice, A., 2003, A Wide-Band Approach to Absolute Phase Retrieval in SAR Interferometry. *Multidimensional Systems and Signal Processing* **14**, pp. 183-205.

Veneziani, N. and Giacovazzo, V.M., 2006, A Multi-Chromatic Approach to SAR Interferometry. Differential Analysis of Interferograms at Close Frequencies in the Spatial Domain and Frequency Domain. In *Proceedings of the International Geoscience & Remote Sensing Symposium (IGARSS'06)*, pp. 3706-3709.

Zebker, H.A. and Villasenor, J., 1992, Decorrelation in Interferometric Radar Echoes. *IEEE Transactions in Geosciences and Remote Sensing*, **30**(5), pp. 950-959.